Calculation of cellular S-values

Author: Roberto González Vegas
Facultat de Física, Universitat de Barcelona, Diagonal 645, 08028 Barcelona, Catalonia, Spain.

Advisor: José M. Fernández-Varea

Abstract: In nuclear medicine, an S-value is defined as the mean absorbed dose to a target volume per nuclear decay in the source region. In this TFG, S-values for cellular dosimetry have been calculated for simplified source/target configurations. Monoenergetic electrons and radionuclides that emit electrons or positrons were considered. Two approaches were adopted to perform the calculations. The present results were compared with literature data computed by full Monte Carlo simulations as well as reference values.

I. INTRODUCTION

Targeted radionuclide therapy is an oncological treatment modality that employs radiopharmacons to specifically deliver ionizing radiation to the tumour. These compounds are generally designed as theranostic agents: when the cancer-specific vector is combined with a suitable radionuclide, the emitted radiations contribute to eradicate the tumour and also to obtain medical images, e.g. by positron emission tomography or single-photon emission computed tomography [1]. The radionuclides that have been proposed for this radiotherapeutic modality have a large yield of Auger (and Coster–Kronig) electrons. These electrons are emitted as a result of the filling of an atomic inner-shell vacancy produced in the course of the nuclear decay. These low-energy electrons have a very short penetration ($\sim$ 0.1–10 μm) in tissue. A large energy deposition is then produced in the vicinity of the decay site while healthy tissues are spared.

In this context, dosimetry at the cellular level has become essential, so that reliable dose calculation methods are needed. The objective of this TFG was to compute cellular S-values, which are the certrepiece of the standard formalism of dose estimation. Monoenergetic electrons and radionuclides emitting electrons or positrons were considered for different source and target combinations. The results were compared with literature data.

II. MIRD FORMALISM

The Medical Internal Radiation Dose (MIRD) committee within the Society of Nuclear Medicine develops methods, models and assumptions to standardize and assess internal radiation dosimetry when a radiopharmacon is administered to a patient. The concept of cellular S-value was introduced by MIRD [2] as a useful quantity to estimate the absorbed dose at the cellular level, being especially helpful when the radiation source is distributed within the cell.

The MIRD scheme proceeds as follows. A certain source region S contains the radionuclide of interest, which is distributed homogeneously. The corresponding cumulated activity $\widetilde{A}$ in the time interval (t_1, t_2) produces a mean absorbed dose $\overline{D}$ to the target volume T (usually the cell nucleus). Since $\overline{D} \propto \widetilde{A}$ we can write [3]

$$\overline{D} = \widetilde{A}\, S(\mathrm{T} \leftarrow \mathrm{S}), \qquad \widetilde{A} = \int_{t_1}^{t_2} A(t)\, \mathrm{d}t, \tag{1}$$

where the proportionality constant is called S-value. For a polyenergetic radiation source that emits up to n particles through various decay modes, the S-value is [3]

$$S(\mathrm{T} \leftarrow \mathrm{S}) = \sum_{i=1}^{n} \frac{\Delta_i\, \phi_i(\mathrm{T} \leftarrow \mathrm{S})}{m_\mathrm{T}}, \tag{2}$$

where Δ_i is the mean energy per nuclear transition of the i-th radiation component, and $\phi_i(\mathrm{T} \leftarrow \mathrm{S})$ is the corresponding fraction of energy emitted from the source region that is absorbed in the target volume, whose mass is m_T. A straightforward calculation of cellular S-values with Eq. (2) can be done using a general-purpose Monte Carlo (MC) code for radiation transport that directly outputs $\overline{D}/\widetilde{A}$.

The considered geometrical model of the cell is represented in Fig. 1. It consists of two concentric spheres of radii R_C and R_N, which correspond to the radii of the cell and its nucleus, respectively. The nucleus and cytoplasm as well as the medium around the cell are supposed to be made of liquid water ($\rho = 1\ \mathrm{g\,cm^{-3}}$).

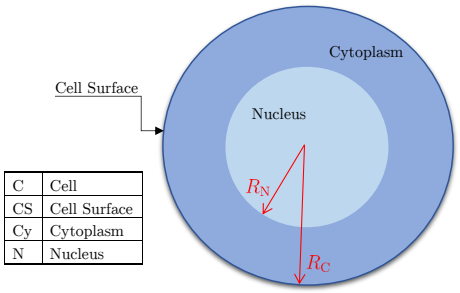

FIG. 1: MIRD cellular model.

More realistic geometries such as ellipsoidal cells and/or eccentric cell-nucleus arrangements can be studied, but they require MC simulations to compute the S-values, which is beyond the aim of this TFG.

A. Dose point kernel method

MC simulations can be a time-consuming method to calculate the S-values. Moreover, a separate simulation is needed for each cell geometry. Eq. (2) can be implemented more efficiently with a calculation method based on dose point kernels (DPKs). In this approach, a point isotropic source is immersed in an infinite, homogeneous medium of liquid water, located at a certain $\vec{r}_0$. This point will be the source of radiation, emitting monoenergetic electrons of energy E. If a target volume T is placed in the medium, a certain fraction of energy emanated by the point source will be deposited in T, denoted as $\phi(\mathrm{T} \leftarrow \vec{r}_0)$. If an extended source region S is placed in the medium, any point in S can be regarded as an independent radiation emitter, contributing with the corresponding fraction of energy to the total absorbed dose $\overline{D}$ to T. Summing up all the possible point sources from the source region, the expression for the S-value is then [3]

$$S(\mathrm{T} \leftarrow \mathrm{S}) = \frac{1}{m_\mathrm{T}} \int_0^\infty 4\pi r^2 \, \rho \, D(r) \, \psi_{\mathrm{T}\leftarrow\mathrm{S}}(r) \, \mathrm{d}r, \qquad (3)$$

where ρ is the mass density of the medium (liquid water) and $D(r)$ is the radial dose distribution (the absorbed dose at a distance r from the source) [13]. The subintegrand includes the function $\psi_{\mathrm{T}\leftarrow\mathrm{S}}(r)$, known as the geometric reduction factor (GRF). This function is the probability that a vector of length r starting from a random point in the source region and randomly oriented ends within the target volume. A graphical representation of the GRF is depicted in Fig. 2.

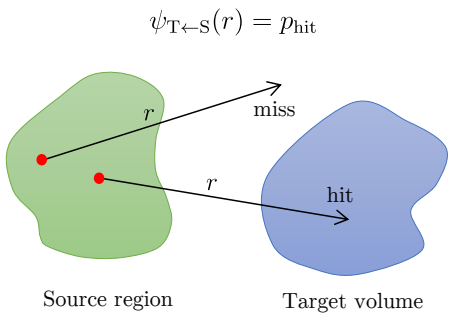

FIG. 2: Representation of the GRF.

The GRFs are analytical for spherical concentric geometries, including the following T ← S combinations: N ← N, N ← Cy, N ← CS, C ← CS and C ← C. For example, taking the cell nucleus as the target volume and assuming that the activity is uniformly distributed also within the cell nucleus, the GRF reads as [3]

$$\psi_{\mathrm{N}\leftarrow\mathrm{N}}(r) = \begin{cases} 1 - \frac{3}{4}\frac{r}{R_\mathrm{N}} + \frac{1}{16}\left(\frac{r}{R_\mathrm{N}}\right)^3 & \text{if } 0 \le r \le 2R_\mathrm{N}, \\ 0 & \text{otherwise.} \end{cases} \qquad (4)$$

B. Continuous-slowing-down approximation

To drastically simplify the calculation of $D(r)$ one can adopt the continuous-slowing-down approximation (CSDA). If electrons are supposed to travel a certain range before being stopped, the energy deposited along the distance advanced will be given by the electronic stopping power $S_\mathrm{el}(E)$. An additional assumption is that electron paths are straight lines. The expression for the S-value in the CSDA is [3]

$$S(\mathrm{T} \leftarrow \mathrm{S}) = \frac{1}{m_\mathrm{T}} \int_0^{X(E)} \left.\frac{\mathrm{d}E}{\mathrm{d}X}\right|_{X(E)-r} \psi_{\mathrm{T}\leftarrow\mathrm{S}}(r) \, \mathrm{d}r, \qquad (5)$$

where $X(E)$ is the range of the electron in the CSDA, and $\mathrm{d}E/\mathrm{d}X|_{X(E)-r}$ is $S_\mathrm{el}(E)$ evaluated at the residual CSDA range of the electron after travelling a distance r across the medium. The tabulated MIRD S-values were calculated with this approximation, and the $S_\mathrm{el}(E)$ used by the committee was experimentally determined by Cole and improved by Howell et al. [3].

III. RESULTS AND DISCUSSION

A. Comparison of DPKs

We define the DPK in the CSDA as

$$4\pi r^2 \, D(r) = \frac{S_\mathrm{el}\big(E(r)\big)}{\rho} = \frac{1}{\rho}\left.\frac{\mathrm{d}E}{\mathrm{d}X}\right|_{X(E)}. \qquad (6)$$

Unlike the CSDA, MC simulations do consider the stochastic character of radiation transport. That is, fluctuations in the energy loss of electrons (energy straggling) and angular deflection caused by elastic collisions are accounted for. This can be seen in Fig. 3, where the presently-calculated CSDA DPKs of monoenergetic 1, 10 and 100 keV electrons in liquid water are compared to the corresponding MC $D(r)$ histograms. The latter were calculated with the PENELOPE MC code [4]. As shown, the CSDA DPKs drop to zero abruptly at the CSDA range, whereas the MC DPKs decrease smoothly and have a non-zero contribution beyond the CSDA range due to the stochastic inelastic processes. That is, electrons are able to deposit some energy farther. The same behaviour is exhibited by the MC DPKs computed with various MC codes [5].

As the objective of this TFG was to compute cellular S-values using only analytical expressions, calculations were performed by numerical integration of Eqs. (3) and (5), specifically using Simpson's 1/3 rule. In this case, the uncertainties corresponding to the integration method were much smaller than the obtained S-values, therefore they are not included in the report. The studied T ← S pairs were N ← N, N ← Cy and N ← CS, since the additivity property of S-values permits obtaining the other possible combinations.

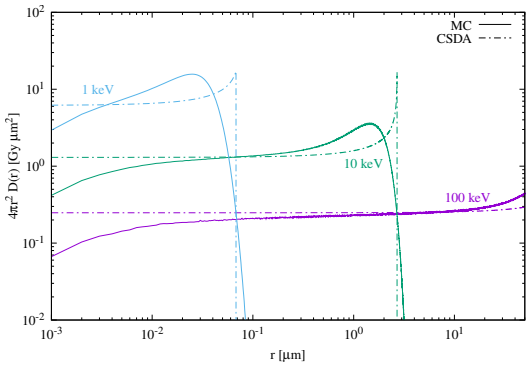

FIG. 3: CSDA (dot-dashed curves) and MC (continuous curves) DPKs for 1, 10 and 100 keV monoenergetic electrons.

The expression recommended by the International Commission of Radiation Units and Measurements (ICRU) for the stopping power of electrons and positrons is the relativistic Bethe formula [6]. Fig. 4 displays the Bethe and Cole formulas for $S_{\mathrm{el}}(E)$. The implications of a better electronic stopping power on the calculated S-values deserves being investigated.

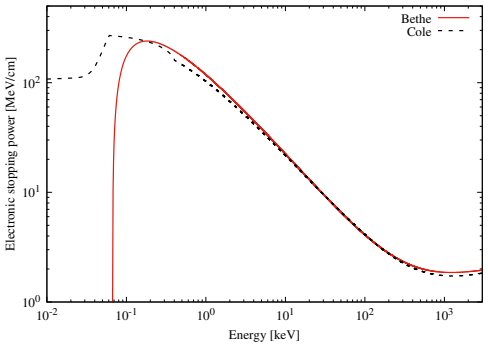

FIG. 4: Bethe and Cole formulas for the electronic stopping power of electrons in liquid water.

B. S-values for monoenergetic electrons

S-values for monoenergetic electrons in the CSDA were calculated for energies ranging from 1 keV to 3 MeV, for the combinations $(R_{\mathrm{C}}, R_{\mathrm{N}}) = (10, 5)$ μm and $(3, 2)$ μm. On the other hand, up to 39 $(R_{\mathrm{C}}, R_{\mathrm{N}})$ arrangements were computed with the DPK method for energies ranging from 1 to 300 keV because the MC radial dose distributions $D(r)$ were not available for higher energies.

The results for monoenergetic electrons calculated with the CSDA are in excellent agreement with the MIRD S-values, as their discrepancies were less than 1% for the three T $\leftarrow$ S arrangements. However, larger differences are encountered for the DPK S-values if compared to the previous, specially for the N $\leftarrow$ CS combination, as shown in Fig. 5 where S-values for the three target-source combinations with the same cellular dimensions are compared. MIRD only tabulates the values for energies above 6 and 16 keV for $(R_{\mathrm{C}}, R_{\mathrm{N}}) = (3, 2)$ μm and $(10, 5)$ μm, respectively. For lower energies, the $S(\mathrm{N} \leftarrow \mathrm{CS})$ values drop to zero; this behaviour can also be observed for the CSDA S-values computed in this TFG, whilst this is not exhibited by the calculations with the DPK method. These discrepancies can be associated to CSDA and MIRD approaches, which disregard both energy straggling and crooked trajectories of electrons, assuming straight paths. As an example, the CSDA range of 10 keV electrons using Cole's expression is ≈ 2.7 μm, which is smaller than the distance from the

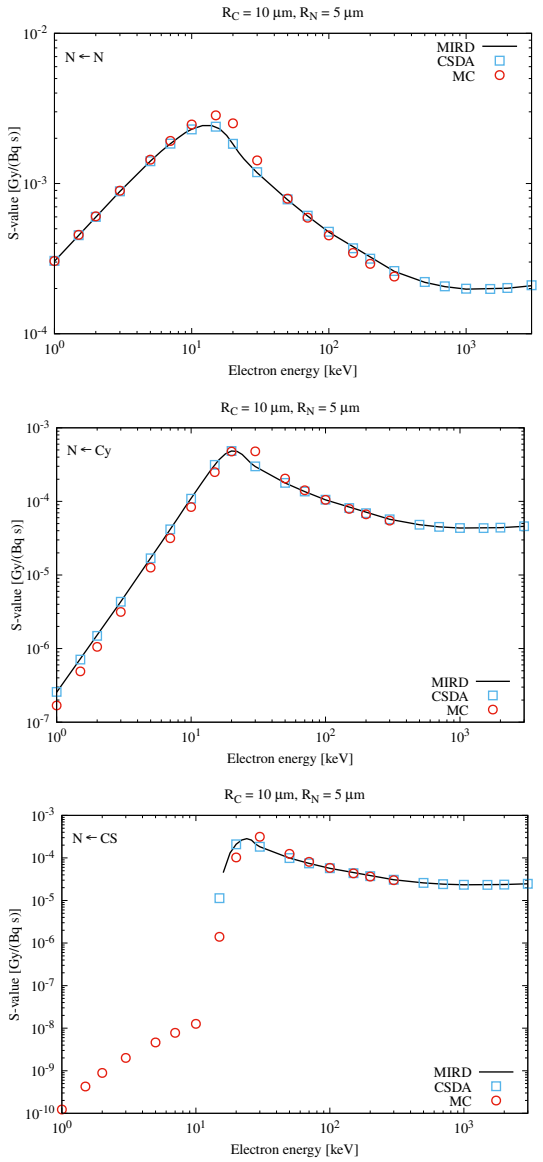

FIG. 5: S-values of monoenergetic electrons for the geometries (top to bottom) N $\leftarrow$ N, N $\leftarrow$ Cy and N $\leftarrow$ CS. The black, continuous curves correspond to the MIRD reference data. The blue squares and red circles are the present S-values calculated with the CSDA and MC DPKs, respectively.

radiation source (CS) to the target (N) for $(R_C, R_N) = (10, 5)$ μm, i.e. $R_C - R_N = 5$ μm, showing that these electrons cannot deposit energy in N. In contrast, electrons with $E > 15$ keV have CSDA ranges larger than 5 μm, ergo some energy will be deposited in the target volume. Conversely, as the $D(r)$ distributions were computed with MC simulations and the stochastic properties of radiation transport are accounted for, the results using the DPK method are in better agreement with the S-values computed by full MC simulations using the PENELOPE code [7].

C. Contribution of $\beta^{\pm}$ particles to the S-values

The contribution to the S-values of β particles was calculated with both DPK method and CSDA for two β^+ radionuclides, namely ^{89}Zr and ^{90}Nb. MIRD does not provide reference values for these radionuclides. Hence, the present results can only be compared with those of Ref. [4] obtained from full MC simulations.

Regarding the DPK method, the contribution to S-values was computed as described in the previous section. However, the implementation of the CSDA was not as straightforward as before because $\beta^{\pm}$ decay is a process that involves three particles in the final state (the daughter nucleus, the emitted electron or positron and an electronic antineutrino or neutrino). As a result, the energy distribution (called Fermi spectrum) is not discrete but continuous. The spectrum ranges from zero up to an end-point energy that corresponds to the maximum kinetic energy of the $\beta^{\pm}$ particle. As an example, Fig. 6 shows the AE+CK+IE and Fermi spectra of ^{90}Nb, containing both discrete and continuous spectra of the aforementioned particles. The FERMI subroutine [8] was used to build the weighted Fermi spectrum of the two radionuclides. This subroutine computes the unnormalised Fermi spectrum of a β emitter, which is indicated as the input, using the Fermi theory of β decay. Then, a double numerical integration is required to obtain the S-values: one corresponding to Eq. (5), and the second weighting the energy spectrum with the probabilities yielded by FERMI, that were normalised beforehand.

Comparing the DPK and CSDA contributions, those obtained from the latter approximation were always overestimated, with differences less than 10%, except for the N ← N target-source configuration, showing slightly larger discrepancies for the smaller cell and cell nucleus radii. For instance, Table I includes the DPK and CSDA contribution to S-values, along with those obtained by full MC simulation using PENELOPE [4], showing great agreement between them. The variations can be ascribed to the disregard of the stochastic processes of radiation transport in the CSDA, and also to the decay scheme used by the FERMI subroutine, which may differ from the nuclear data employed in the calculation of $D(r)$ and PENELOPE S-values. The contribution of the β particles to the total S-value (including Auger, Coster–Kronig and internal conversion electrons) was also analysed, resulting in an excellent agreement of both considered methods with PENELOPE data. The CSDA slightly overestimates the total contribution for the N ← N configuration, and the largest contributions were found for S(N ← CS) values, even exceeding a 50% for ^{89}Zr.

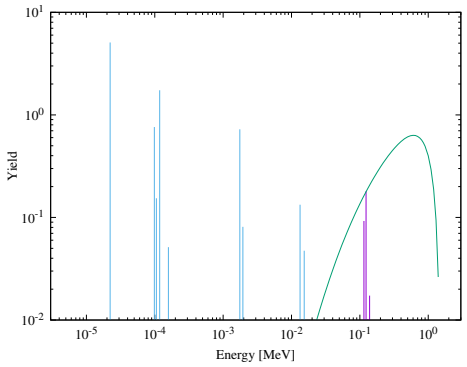

FIG. 6: Yield of Auger and Coster–Kronig (blue) and internal conversion (magenta) electrons of ^{90}Nb. The Fermi spectrum (green) of its β^+ particles is also depicted.

TABLE I: Present DPK and CSDA partial S-values and those obtained with the PENELOPE code for the positrons emitted in the β^+ decay of ^{89}Zr and ^{90}Nb for the indicated target-source configurations and (R_C, R_N).

Radionuc.	(R_C, R_N) (μm, μm)		S(N ← N) Gy/(Bq s)	S(N ← Cy) Gy/(Bq s)	S(N ← CS) Gy/(Bq s)
^{89}Zr	(3, 2)	CSDA	3.80×10^{-4}	1.30×10^{-4}	8.36×10^{-5}
		DPK	3.39×10^{-4}	1.20×10^{-4}	7.83×10^{-5}
		MC	3.81×10^{-4}	1.12×10^{-4}	8.12×10^{-5}
^{89}Zr	(10, 5)	CSDA	6.09×10^{-5}	1.33×10^{-5}	7.20×10^{-6}
		DPK	5.63×10^{-5}	1.29×10^{-5}	7.11×10^{-6}
		MC	5.70×10^{-5}	1.30×10^{-5}	7.08×10^{-6}
^{90}Nb	(3, 2)	CSDA	7.63×10^{-4}	2.60×10^{-4}	1.68×10^{-4}
		DPK	6.73×10^{-4}	2.37×10^{-4}	1.55×10^{-4}
		MC	6.90×10^{-4}	2.33×10^{-4}	1.53×10^{-4}
^{90}Nb	(10, 5)	CSDA	1.22×10^{-4}	2.67×10^{-5}	1.44×10^{-5}
		DPK	1.11×10^{-4}	2.54×10^{-5}	1.39×10^{-5}
		MC	1.06×10^{-4}	2.57×10^{-5}	1.35×10^{-5}

D. S-values for radionuclides

Finally, S-values for 12 Auger-emitting radionuclides were calculated. Generally, the S-values calculated with the DPK method were in good agreement with those computed with the CSDA when the target-source configuration is N ← N, i.e. when both volumes are overlapped, with DPK values being underestimated as a rule. Furthermore, the differences have a tendency to decrease as R_N increases. Nevertheless, the largest discrepancies between the presently-calculated S-values were encountered for the N ← CS arrangement, whilst N ← Cy differences

were somehow in between the previous combinations. In addition, results for ^{99m}Tc showed better agreement between both values than the other radionuclides.

TABLE II: Presently-calculated, PENELOPE and MIRD S-values of different radionuclides for $(R_C, R_N) = (3, 2)$ μm.

Radionuc.	S-value	DPK	PENELOPE	CSDA	MIRD
	T ← S	Gy/(Bq s)	Gy/(Bq s)	Gy/(Bq s)	Gy/(Bq s)
^{67}Ga	N ← N	2.57×10^{-2}	2.57×10^{-2}	2.35×10^{-2}	2.29×10^{-2}
	N ← Cy	3.21×10^{-3}	3.21×10^{-3}	3.74×10^{-3}	3.59×10^{-3}
	N ← CS	7.09×10^{-4}	7.16×10^{-4}	1.43×10^{-3}	1.38×10^{-3}
^{99m}Tc	N ← N	1.18×10^{-2}	1.18×10^{-2}	1.16×10^{-2}	1.19×10^{-2}
	N ← Cy	3.51×10^{-4}	3.52×10^{-4}	3.47×10^{-4}	3.46×10^{-4}
	N ← CS	1.71×10^{-4}	1.70×10^{-4}	1.30×10^{-4}	1.29×10^{-4}
^{111}In	N ← N	1.93×10^{-2}	1.93×10^{-2}	1.91×10^{-2}	1.91×10^{-2}
	N ← Cy	1.16×10^{-3}	1.14×10^{-3}	1.05×10^{-3}	1.12×10^{-3}
	N ← CS	6.42×10^{-4}	6.39×10^{-4}	4.43×10^{-4}	4.50×10^{-4}

On the other hand, the present CSDA S-values are in excellent agreement with the MIRD tables, whereas the DPK data generally differ from MIRD S-values by less than 10% for the N ← N arrangement, and larger discrepancies are observed as the target volume is farther with respect to the source region. Conversely, PENELOPE and present DPK S-values are in excellent agreement, with differences below 2% for the three T ← S arrangements. Table II shows the DPK and CSDA S-values of three radionuclides being compared with MIRD and PENELOPE data. As mentioned, MIRD and CSDA S-values are in better agreement between them, ocurring the same for PENELOPE and DPK data.

IV. CONCLUSIONS

In this project, cellular S-values have been calculated by numerical integration and compared with the literature data. MIRD reference tabulations were matched in good agreement with the present results, especially when the CSDA was used. Generally, the S-values calculated with the DPK method were in better agreement with simulated data that employed MC codes of radiation transport, as the $D(r)$ used were indeed computed with these algorithms. Furthermore, future work will compare the present and MIRD S-values with new ones computed with the relativistic Bethe formula for the $S_{\rm el}(E)$, which is the expression recommended by the ICRU.

The use of Auger electrons in therapeutic modalities is a relatively unexplored field, with lot of work to be done [9, 10]. Current interests include computing S-values for more realistic ellipsoidal cell geometries and eccentric cell-nucleus arrangements [11, 12], as cell geometry can influence not only the single-cell S-values, but also the crossfire to adjacent cells, especially for the low-range Auger electrons [4].

Acknowledgments

I am indebted to my advisor José M. Fernández-Varea for his guidance and help during the development of this project. I am also grateful to my family and friends for their unconditional support during these years.

[1] Bavelaar, B. M., Lee, B. Q., Gill, M. R., Falzone, N., & Vallis, K. A. (2018). Subcellular targeting of theranostic radionuclides. *Frontiers in Pharmacology* **9**, 996.

[2] Loevinger, R., Budinger, T. & Watson, E. (1988). MIRD Primer for Absorbed Dose Calculations. *Society of Nuclear Medicine*.

[3] Goddu, S. M., Howell, R. W. and Bouchet, L. G. & Rao, D. V. (1997). MIRD cellular S values. *Reston, VA: Society of Nuclear Medicine*.

[4] Falzone, N., Fernández-Varea, J. M., Flux, G., & Vallis, K. A. (2015). Monte Carlo evaluation of Auger electron-emitting theranostic radionuclides. *Journal of Nuclear Medicine* **56**, 1441–1446.

[5] Mendes, B. M., Guimarães-Antunes, P. C., Soares Lopes Branco, I., do Nascimento, E., Seniwal, B., Ferreira-Fonseca, T. C. & Yoriyaz, H. (2021). Calculation of dose point kernel values for monoenergetic electrons and beta emitting radionuclides: Intercomparison of Monte Carlo codes. *Radiation Physics and Chemistry* **181**, 109327.

[6] Berger, M. J., Inokuti, M., Anderson, H. H., Bichsel, H., Dennis, J. A., Powers, D., Seltzer, S. M. & Turner, J. E. (1984). Report 37 *Journal of the International Commission on Radiation Units and Measurements*, **os19**.

[7] Hubert, S. (2009). Tools for the Monte Carlo calculation of cellular S-values (MSc Thesis). KTH School of Technology and Health, Stockholm.

[8] García-Toraño, E., Peyres, V., Bé, M.-M., Dulieu, C., Lepy, M.-C. & Salvat, F. (2017). Simulation of decay processes and radiation transport times in radioactivity measurements. *Nuclear Instruments and Methods in Physics Research B* **396**, 43–49.

[9] Ku, A., Facca, V. J., Cai, Z., & Reilly, R. M. (2019). Auger electrons for cancer therapy – a review. *EJNMMI radiopharmacy and chemistry* **4**, 27.

[10] Howell, R. W. (2020). Advancements in the use of Auger electrons in science and medicine during the period 2015–2019. *International Journal of Radiation Biology*, 1–26.

[11] Salim, R. & Taherparvar, P. (2019). Monte Carlo single–cell dosimetry using Geant4-DNA: the effects of cell nucleus displacement and rotation on cellular S values. *Radiation and Environmental Biophysics* **58**, 353–371.

[12] Šefl, M., Incerti, S., Papamichael, G. & Dimitris Emfietzoglou (2015). Calculation of cellular S-values using Geant4-DNA: The effect of cell geometry. *Applied Radiation and Isotopes* **104**, 113–123.

[13] The $D(r)$ histograms used in this project were calculated by advisor J.M. Fernández-Varea using PENELOPE.